

# Chiral behaviour of the pion decay constant in $N_f = 2$ QCD

---



**Stefano Lottini\***

*NIC, DESY – Platanenallee 6, 15738 Zeuthen, Germany*

*E-mail: [stefano.lottini@desy.de](mailto:stefano.lottini@desy.de)*

**for the ALPHA Collaboration**

As increased statistics and new ensembles with light pions have become available within the CLS effort, we complete previous work by inspecting the chiral behaviour of the pion decay constant. We discuss the validity of Chiral Perturbation Theory ( $\chi$ PT) and examine the results concerning the pion decay constant and the ensuing scale setting, the pion mass squared in units of the quark mass, and the ratio of decay constants  $f_K/f_\pi$ ; along the way, the relevant low-energy constants of SU(2)  $\chi$ PT are estimated. All simulations were performed with two dynamical flavours of nonperturbatively O(a)-improved Wilson fermions, on volumes with  $m_\pi L \geq 4$ , pion masses  $\geq 192$  MeV and lattice spacings down to 0.048 fm. Our error analysis takes into account the effect of slow modes on the autocorrelations.

DESY 13-213

*31st International Symposium on Lattice Field Theory LATTICE 2013*

*July 29 – August 3, 2013*

*Mainz, Germany*

---

\*Speaker.

## 1. Introduction

The nonperturbative features of quantum chromodynamics (QCD) are more and more prominent as one approaches the low-energy regime; there, the most successful strategy to determine its properties is, to date, numerical simulation on the lattice, complemented by insight provided by chiral perturbation theory ( $\chi$ PT) as to how the chiral limit is reached.

In the past years, new  $N_f = 2$  ensembles have been produced within the Coordinated Lattice Simulations (CLS) effort, closer and closer to both the physical point and the continuum limit. Here we report on the chiral behaviour of the pion decay constant  $f_\pi$  (and related quantities) obtained from the latest set of CLS ensembles, and the subsequent determinations of the  $SU(2)$   $\chi$ PT low-energy constants involved. The analysis presented here can be seen as a complement to Ref. [1] (to which we refer for most of the setup details), where analogous investigations were carried on, among other topics, concerning the kaon decay constant  $f_K$ .

All ensembles were generated using  $O(a)$ -improved Wilson lattice action with two degenerate dynamical flavours, implementing either Domain-Decomposition [2] or Mass-Preconditioning [3]. Table 1 summarises the relevant information on the ensembles employed in the present analysis.

Two-point functions were measured using 10 to 20  $U(1)$  stochastic sources per configuration, and subsequently used to extract meson- and PCAC-masses and decay constants, as detailed in [1], with a statistical uncertainty on the level of 1% or better. For renormalisation, the  $b$ -factors come from one-loop perturbation theory [4], and the  $Z$ -factors are nonperturbatively determined [1].

## 2. Chiral analyses

In the data analysis, first an independent variable is built, parameterising the approach to the chiral and the physical points; in contrast to the one employed in [1], here we deal with the purely pionic (i.e. light-light flavours) variable

$$y_1 = \frac{m_\pi^2(m_q)}{8\pi^2 f_\pi^2(m_q)}, \quad (2.1)$$

appearing as expansion parameter in the  $\chi$ PT formulae.  $m_\pi$  and  $f_\pi$  are the measured quantities at the finite quark masses; the physical point corresponds to  $y_\pi \simeq 0.01353$ .

Generally, fits are performed, simultaneously for all values of  $\beta$ , to the functional form coming from  $\chi$ PT, taking correlations among measurement into account. Our goal being the chiral and physical points, we inspect fits in the range  $m_\pi \leq m_\pi^{(\text{cut})}$  with  $m_\pi^{(\text{cut})} \leq 650, 500, 390, 345$  MeV; as it turns out, beyond NLO, a quadratic term has to be included for the fit to be stable in  $m_\pi^{(\text{cut})}$ ; systematic uncertainties in the resulting parameters were estimated also by altering the fit functions.

Correlations are propagated down to the final quantities. Special care is taken for the integrated autocorrelation time, by applying the technique developed in [5]: the effects of slow modes in the transition matrix, to which an observable can couple, are estimated by attaching an  $\exp(-t/\tau_{\text{exp}})$  tail, with  $\tau_{\text{exp}}$  coming from prior determinations, to the autocorrelation function where its statistical error is too large for direct determination. For all quantities, however, the largest contribution (about 30 to 60%) to the full uncertainty comes from the error on the renormalisation factor  $Z_A$ .

$\beta = 5.2$ ( $a \simeq 0.075$ fm)				$\beta = 5.3$ ( $a \simeq 0.065$ fm)				$\beta = 5.5$ ( $a \simeq 0.048$ fm)			
	$m_\pi$	MDU	$\frac{\text{MDU}}{\tau_{\text{exp}}}$		$m_\pi$	MDU	$\frac{\text{MDU}}{\tau_{\text{exp}}}$		$m_\pi$	MDU	$\frac{\text{MDU}}{\tau_{\text{exp}}}$
A2	629	8000	120	E4	580	2496	10	N4	551	3752	4
A3	492	8032	120	E5f	436	16000	60	N5	440	3808	4
A4	383	8096	120	E5g	436	16000	120	N6	340	8040	40
A5	330	4004	160	F6	311	4800	36	O7	267	3920	20
B6	281	1272	50	F7	266	9416	70				
				G8	192	1114	20				

**Table 1:** Overview of the ensembles used. For the three bare lattice couplings  $\beta$ , three quantities are shown: approximate pion mass (expressed in MeV), ensemble extent in Molecular Dynamic Units (MDU), and the latter in units of the autocorrelation time associated to the slowly-decaying modes (see text). For each ensemble 10 stochastic sources were used to extract the two-point functions, except for the last entry of each  $\beta$  (20 sources). All ensembles have  $m_\pi L \geq 4$  and time extent  $T = 2L$ . The two ‘E5’ ensembles differ in the trajectory length (respectively  $\tau = 0.5$  and 2.0 MDU).

## 2.1 Analysis of $f_\pi$

Here and in the following, we denote decay constants in lattice units with an uppercase symbol, as in  $F_\pi(\beta) = a(\beta)f_\pi$ , with  $f_\pi$  taking the value  $f_\pi^{\text{phys}} = 130.4$  MeV at the physical point. The outcome of this study, focused on how and to which extent can  $\chi$ PT be trusted to describe the behaviour of  $f_\pi$ , will then provide a scale-setting prescription.

The main fits are performed to the  $\chi$ PT NLO functional [6], plus a quadratic term:

$$F_\pi(y_1) = F_\pi^{\text{phys}}(\beta) \{1 + \alpha_4(y_1 - y_\pi) - y_1 \log y_1 + y_\pi \log y_\pi + B(y_1 - y_\pi)^2\} , \quad (2.2)$$

where the three  $F_\pi$  (one for each  $\beta$ ) will yield the scale setting and  $\alpha_4$  encodes the  $SU(2)$  NLO low-energy constant (LEC)  $\bar{\ell}_4$ :

$$\bar{\ell}_4 = \log \frac{\Lambda_4^2}{\mu^2} \Big|_{\mu \leftarrow m_\pi^{\text{phys}} = 134.8 \text{ MeV}} ; \quad \bar{\ell}_4 = \frac{\alpha_4}{1 - \alpha_4 y_\pi + y_\pi \log y_\pi} - \log y_\pi . \quad (2.3)$$

This functional form fits the data in a stable way for various  $m_\pi^{(\text{cut})}$  (Fig. 1, left), and we take the results from the cut at 500 MeV as median value; systematic uncertainties come from comparing functional forms without  $B$  and/or the chiral logarithms. The absence of  $am_q$ -effects is illustrated by the collapse-plot of Fig. 1, right top, where data for each  $\beta$  are rescaled to a common curve. An important remark is the following: the result we get for  $B$  is such that, in the data range, the  $y_1^2$ -term contributes by as much as  $\sim 15\%$  to the curve. This is reflected in Fig. 1, right bottom, that illustrates the behaviour of  $\alpha_4$  as a function of the pion-mass cut.

This procedure leads to the following determination of the lattice spacing  $a(\beta)$ , compatible with the one of [1] albeit slightly smaller in central value (the first error is statistical, the second systematic):

$$a(5.2) = 0.0750(9)(10) \text{ fm} , \quad a(5.3) = 0.0652(6)(7) \text{ fm} , \quad a(5.5) = 0.0480(5)(5) \text{ fm} . \quad (2.4)$$

This is also compatible with an update of [1], based on  $f_K$  and including all new ensembles.

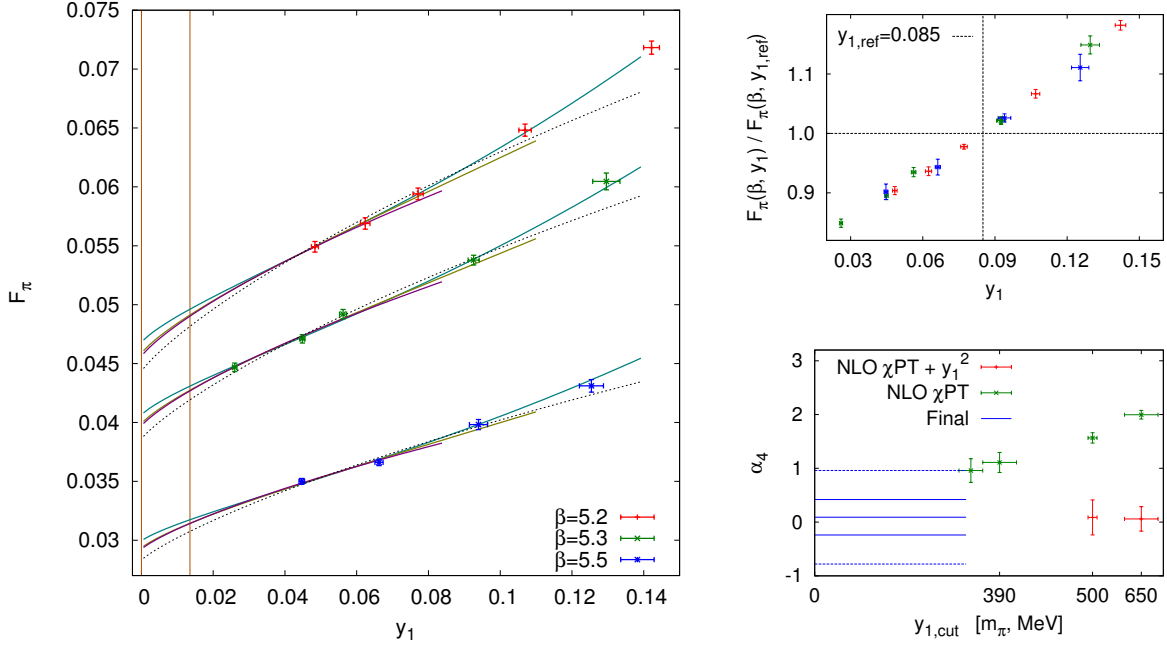


**Figure 1:** Behaviour of  $F_\pi$ . *Left:*  $F_\pi(y_1)$ , measured points at the three  $\beta$  and fit to Eq. 2.2 for  $m_\pi^{(\text{cut})} = 500, 390, 345$  MeV (solid lines); the dashed line is a fit with  $B = 0$  and  $m_\pi^{(\text{cut})} = 500$  MeV added for illustration. The vertical line marks  $y_\pi$ . *Right, top:* collapse-plot of the same data, rescaled to the corresponding interpolated  $F_\pi(y_{1,\text{ref}} = 0.085)$  (same colours as in left plot). *Right, bottom:* resulting fit parameter  $\alpha_4$  for the fit with and without quadratic term for various  $m_\pi^{(\text{cut})}$ ; horizontal lines mark mean value, one-sigma statistical error band, and systematic uncertainty of the final result (equivalent to  $\bar{\ell}_4$  of Eq. 2.5). Note how the ‘NLO  $\chi$ PT +  $y_1^2$ ’ points are stable at the value suggested by the  $m_\pi^{(\text{cut})} \rightarrow 0$  trend of the ‘NLO  $\chi$ PT’ points.

Another relevant quantity is the ratio between  $f_\pi$  at the physical- and chiral-points, which – to NLO – encodes directly the LEC  $\bar{\ell}_4$ :

$$\frac{f_\pi}{f} = 1.061(6)(16) \quad ; \quad \bar{\ell}_4 = 4.4(4)(9) \quad ; \quad (2.5)$$

the former falls within the  $N_f = 2$  world average by the 2013 FLAG review [7].

On a related note, we mention that a continuum-extrapolation of  $f_\pi r_0$ , done in a similar fashion, yields for the hadron parameter  $r_0$  a slightly smaller (but still compatible) value than presented in [1]:  $r_0 = 0.485(7)(7)$  fm.

## 2.2 Analysis of $m_\pi^2/M_R$

We now turn to the ratio of the squared pion mass to the (renormalised) quark mass  $M_R$ , expressed, as the chiral condensate below, in the  $\overline{\text{MS}}$  scheme at a scale  $\mu = 2$  GeV. The  $\chi$ PT NLO expression extends the Gell-Mann-Oakes-Renner (GMOR) relation [8] to:

$$\frac{m_\pi^2}{4M_R} \Big|_{\text{NLO}} = \frac{\Sigma_0}{f^2} \left\{ 1 + \alpha_3 y_1 + \frac{1}{2} y_1 \log y_1 \right\} \quad , \quad (2.6)$$

with the linear coefficient  $\alpha_3$  encoding the NLO low-energy constant  $\bar{\ell}_3|_{\text{NLO}} = -2\alpha_3 - \log y_\pi$ .

One is primarily interested in extracting an estimate for the chiral condensate  $\Sigma_0$  in the continuum limit: with this goal in mind, we encode the expected  $a^2$ -scaling directly in the overall amplitude of the above formula, and look for the (third root of the) condensate in units of the physical pion decay constant. We also allow for the usual NNLO analytic term in the fit function:

$$\frac{m_\pi^2}{4M_R} = \left[ (S_0 + a^2 S_1) \frac{F_{\pi,\text{phys}}^3}{F^2} \right] \left\{ 1 + \alpha_3 y_1 + \frac{1}{2} y_1 \log y_1 + B y_1^2 \right\} ; \quad \sqrt[3]{\Sigma_{0,\text{cont}}} = f_{\pi,\text{phys}} \sqrt[3]{S_0} ; \quad (2.7)$$

(the validity of the Ansatz of  $a^2$ -scaling is corroborated by variants of the analysis in which first a  $\beta$ -dependent amplitude is obtained, then the continuum limit is taken; the values of  $a^2$  used here are those coming from the  $f_\pi$ -based scale setting).

Eq. 2.7 describes well the data, which lie approximately flat in  $y_1$  (Fig. 2, left), and the value of  $S_0$  is stable against the usual variants of the fit procedure;  $\alpha_3$ , on the other hand, is more pion-mass-cut- and fit-function-dependent, leading to a large systematic error on  $\bar{\ell}_3$ . From the fit to the above equation, with  $m_\pi^{(\text{cut})} = 500$  MeV, we get the following values:

$$\sqrt[3]{\Sigma_{0,\text{cont}}} = 268.1(2.6)(4.9) \text{ MeV} ; \quad \bar{\ell}_3 = 2.4(0.1)_{(-1.3)}^{(+0.7)} . \quad (2.8)$$

The former result compares favorably to most recent two-flavours lattice determinations [9, 10]. We remark that a more first-principle lattice determination of  $\Sigma_0$ , minimally relying on  $\chi$ PT assumptions, is currently being carried on [11] based on the method proposed in [12] and using the same CLS configurations employed here; the same approach, in the context of twisted-mass fermions, is pursued in Ref. [10], with an outcome which overshoots slightly what found here – by about 1.5 standard deviations) – once recast as  $r_0 \sqrt[3]{\Sigma_0}$  (there, this combination is used to overcome current discrepancies in the physical determination of  $r_0$ ).

### 2.3 The ratio $f_K/f_\pi$

We now consider a heavier valence quark and turn to study “kaon” properties, by moving along the trajectory (dubbed ‘strategy 1’ in [1]) defined by  $m_K/f_K = m_K/f_K|_{\text{phys}} \simeq 3.19$ . Partially-quenched  $\chi$ PT dictates the behaviour of the quantity  $f_K/f_\pi$  [13], which in our range is almost linear in  $y_1$ . Nevertheless, as usual, we allow for a  $y_1^2$  term in the fit function:

$$\frac{f_K}{f_\pi} \Big|_{\text{NLO}+y_1^2} = R \left\{ 1 + c_1 y_1 + \frac{y_1}{2} \log y_1 - \frac{y_1}{8} \log \left( 2 \frac{y_K}{y_1} - 1 \right) + c_2 y_1^2 \right\} ; \quad y_K = \frac{m_K^2}{8\pi^2 f_\pi^2} \simeq 0.182 . \quad (2.9)$$

Thanks to the stabilising effect of the ensemble with the lightest pion (G8), the ratio at the physical point can be accurately determined, see Fig. 2, right; moreover, the presence of the quadratic term has an effect similar to that of Fig. 1, bottom right. Adding  $(af_\pi)^2$ -terms as a check did not alter the picture at all. We then quote the result from the fit to the above equation with  $m_\pi^{(\text{cut})} = 500$  MeV, which agrees with most two-flavours lattice estimates, and the CKM matrix element obtained from the latter through the values in [14, 15]:

$$\frac{f_K}{f_\pi} \Big|_{\text{phys}} = 1.1874(57)(30) , \quad |V_{us}| = 0.2263(13) . \quad (2.10)$$

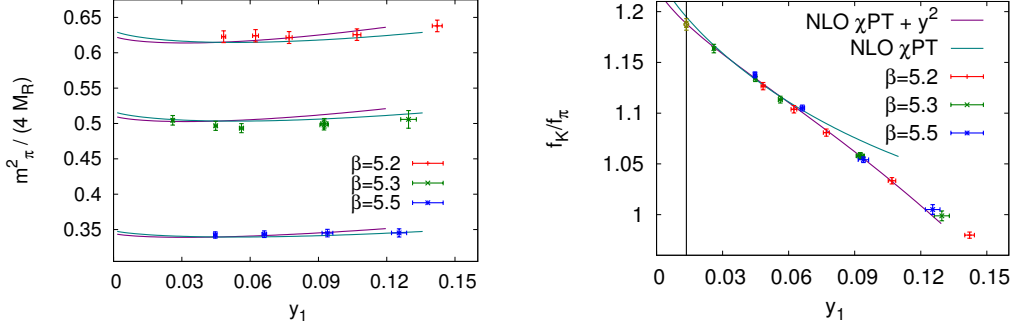


**Figure 2:** *Left:* The quantity  $m_\pi^2/(4M_R)$ . The solid lines show fits to Eq. 2.7 at two pion-mass cuts (390 and 500 MeV). *Right:* Ratio  $f_K/f_\pi$  as a function of  $y_1$ ; the vertical line marks  $y_\pi$  and the solid lines are best-fit curves with and without the  $c_2 y_1^2$  term (and  $m_\pi^{(\text{cut})} = 500$  and 345 MeV respectively).

### 3. Conclusions

This work presents an analysis of the chiral behaviour of pion-related quantities based on two-flavour lattice QCD. The agreement of the lattice spacing determination with the previous ones (from  $f_K$ ) encourages us; compared to the kaon-based analysis, however, here  $m_\pi^4$ -terms are necessary to stabilise the fits. The ubiquitous need for such terms makes one wonder to which extent is  $\chi$ PT-behaviour observed: indeed, their rôle in the fits is to approximately cancel the curvature of the NLO chiral logarithms and restore a roughly linear dependence in a wide range of  $m_\pi^2$ . A possible reading of this finding is that the chiral logarithms set in only beyond the pion masses well probed by our data. Similar observations, namely that the NNLO terms effectively cancel out the NLO logarithms, thus restoring a linear behaviour (e.g. for  $f_\pi$ ), and that linearity sets in at relatively low pion masses already, have been reiterated in the detailed analysis of [16]. The continuum and chiral limits are carefully taken thanks to our ensembles covering a comfortable region in the  $(a, m_\pi)$  plane (in particular, the lightest-pion ensemble G8 seems pivotal for stability).

To complete this preliminary investigation, a similar work on the  $\xi$ -expansion for  $\chi$ PT formulae (i.e. in terms of quark mass instead of pion mass squared), as well as full inclusion of NNLO chiral logarithms, are planned, with the goal of a better assessment of systematic uncertainties; moreover, comparative analyses of the same data, based on the Sommer scale  $r_0$  [17] and on the recently introduced flow-time scale  $t_0$  [18], are currently being undertaken [19]. A more complete and articulated account of the present analysis is deferred to a forthcoming paper.

The authors gratefully acknowledge access to HPC resources in the form of a regular GCS/NIC project<sup>1</sup>, a JUROPA/NIC project<sup>1</sup> and through PRACE-2IP, receiving funding from the European Community’s Seventh Framework Programme (FP7/2007-2013) under grant agreement RI-283493. This work is supported in part by the grants SFB/TR9 of the Deutsche Forschungsgemeinschaft.

<sup>1</sup>See <http://www.fz-juelich.de/ias/jsc/EN/Expertise/Supercomputers/ComputingTime/Acknowledgements.html>.

## References

- [1] P. Fritzsche, F. Knechtli, B. Leder, M. Marinkovic, S. Schaefer, et al., *The strange quark mass and Lambda parameter of two flavor QCD*, *Nucl.Phys.* **B865** (2012) 397–429, [[arXiv:1205.5380](#)].
- [2] M. Lüscher, *Schwarz-preconditioned HMC algorithm for two-flavour lattice QCD*, *Comput.Phys.Commun.* **165** (2005) 199–220, [[hep-lat/0409106](#)].
- [3] M. Marinkovic and S. Schaefer, *Comparison of the mass preconditioned HMC and the DD-HMC algorithm for two-flavour QCD*, *PoS LATTICE2010* (2010) 031, [[arXiv:1011.0911](#)].
- [4] S. Sint and P. Weisz, *Further one loop results in  $O(a)$  improved lattice QCD*, *Nucl.Phys.Proc.Suppl.* **63** (1998) 856–858, [[hep-lat/9709096](#)].
- [5] ALPHA Collaboration, S. Schaefer, R. Sommer, and F. Viotto, *Critical slowing down and error analysis in lattice QCD simulations*, *Nucl.Phys.* **B845** (2011) 93–119, [[arXiv:1009.5228](#)].
- [6] J. Gasser and H. Leutwyler, *Chiral Perturbation Theory to One Loop*, *Annals Phys.* **158** (1984) 142.
- [7] FLAG Working Group, “Review of lattice results concerning low energy particle physics.” <http://itpwiki.unibe.ch/flag>. (Made available as wiki prior to submission).
- [8] M. Gell-Mann, R. Oakes, and B. Renner, *Behavior of current divergences under  $SU(3) \times SU(3)$* , *Phys.Rev.* **175** (1968) 2195–2199.
- [9] B. B. Brandt, A. Jüttner, and H. Wittig, *The pion vector form factor from lattice QCD and NNLO chiral perturbation theory*, [arXiv:1306.2916](#).
- [10] K. Cichy, E. Garcia-Ramos, and K. Jansen, *Chiral condensate from the twisted mass Dirac operator spectrum*, *JHEP* **1310** (2013) 175, [[arXiv:1303.1954](#)].
- [11] G. P. Engel, L. Giusti, S. Lottini, and R. Sommer, *Chiral condensate from the Banks-Casher relation*, *PoS LATTICE2013* (2013) 119, [[arXiv:1309.4537](#)].
- [12] L. Giusti and M. Luscher, *Chiral symmetry breaking and the Banks-Casher relation in lattice QCD with Wilson quarks*, *JHEP* **0903** (2009) 013, [[arXiv:0812.3638](#)].
- [13] S. R. Sharpe, *Enhanced chiral logarithms in partially quenched QCD*, *Phys.Rev.* **D56** (1997) 7052–7058, [[hep-lat/9707018](#)].
- [14] M. Antonelli, V. Cirigliano, G. Isidori, F. Mescia, M. Moulson, et al., *An Evaluation of  $V_{us}$  and precise tests of the Standard Model from world data on leptonic and semileptonic kaon decays*, *Eur.Phys.J.* **C69** (2010) 399–424, [[arXiv:1005.2323](#)].
- [15] J. Hardy and I. Towner, *Superallowed  $0^+ \rightarrow 0^+$  nuclear beta decays: A New survey with precision tests of the conserved vector current hypothesis and the standard model*, *Phys.Rev.* **C79** (2009) 055502, [[arXiv:0812.1202](#)].
- [16] S. Dürr, Z. Fodor, C. Hoelbling, S. Krieg, T. Kurth, et al., *Lattice QCD at the physical point meets  $SU(2)$  chiral perturbation theory*, [arXiv:1310.3626](#).
- [17] R. Sommer, *A New way to set the energy scale in lattice gauge theories and its applications to the static force and alpha-s in  $SU(2)$  Yang-Mills theory*, *Nucl.Phys.* **B411** (1994) 839–854, [[hep-lat/9310022](#)].
- [18] M. Lüscher, *Properties and uses of the Wilson flow in lattice QCD*, *JHEP* **1008** (2010) 071, [[arXiv:1006.4518](#)].
- [19] M. Bruno and R. Sommer, *On the  $N_f$ -dependence of gluonic observables*, *PoS LATTICE2013* (2013) 321, [[arXiv:1311.5585](#)].